Concentration and cavitation in the vanishing pressure limit of solutions to a 3×3 generalized Chaplygin gas equations *

Yu Zhang [1†] Shuai Fan [1] Yanyan Zhang [2]

[1] *Department of Mathematics, Yunnan Normal University, Kunming 650500, PR China*

[2] *College of Mathematics and Statistics, Xinyang Normal University, Xinyang 464000, PR China*

Abstract: The phenomena of concentration and cavitation are identified and analyzed by studying the vanishing pressure limit of solutions to the 3×3 isentropic compressible Euler equations for generalized Chaplygin gas (GCG) with a small parameter. It is rigorously proved that, any Riemann solution containing two shocks and possibly one-contact-discontinuity of the GCG equations converges to a delta-shock solution of the same system as the parameter decreases to a certain critical value. Moreover, as the parameter goes to zero, that is, the pressure vanishes, the limiting solution is just the delta-shock solution of the pressureless gas dynamics (PGD) model, and the intermediate density between the two shocks tends to a weighted δ-measure that forms the delta shock wave; any Riemann solution containing two rarefaction waves and possibly one contact-discontinuity tends to a two-contact-discontinuity solution of the PGD model, and the nonvacuum intermediate state in between tends to a vacuum state. Finally, some numerical results are presented to exhibit the processes of concentration and cavitation as the pressure decreases.

Keywords: Generalized Chaplygin gas equations; Delta shock wave; Concentration and cavitation; Vanishing pressure limit; Numerical simulations.

1. Introduction

It is universally acknowledged that fluids are substances whose molecular structure offers no resistance to external shear forces: even the smallest force causes deformation of a fluid particle. In most cases of interest, a fluid can be regarded as continuum, thus satisfies the balance laws of density, momentum, and energy. However, if the fluid is isentropic, then just the balance laws of density and momentum should be taken into account. In this situation, the pressure, as a thermodynamic variable, only depends on density. Such dependence is usually called as the state equation, which is possible to be estimated from statistic mechanics or kinetic theory and is usually obtained by laboratory measurement.

On the other hand, as stated in [9], in the compressible fluid flow, if the speed is larger than the sound speed, shocks may form when particles collide. However, as observed numerically in

* Supported by NSF of China (11501488), Yunnan Fundamental Research Projects (202101AT070128, 2018FD015) and Scientific Research Foundation Project of Yunnan Education Department (2018JS150).

† Corresponding author. E-mail address: yuzhang13120@126.com (Y. Zhang).

Published by EDP Sciences and available at https://www.mmnp-journal.org or https://doi.org/10.1051/mmnp/2022009

[4, 5, 6] for gas dynamics in the regime of small pressure: for one case, the particles seem to be more sticky and tend to concentrate at some shock locations which move with the associated shock speeds, and for the other case, the particles seem to be far apart and tend to form cavitation in the region of rarefaction waves. Such phenomena may be regarded as a tendency towards the concentration and cavitation in terms of the density.

One of the main objectives of this paper is to show rigorously that the phenomena of concentration and cavitation in the solutions are fundamental and physical in the following 3×3 isentropic compressible Euler equations

$$\begin{cases} \rho_t + (\rho u)_x = 0, \\ (\rho u)_t + (\rho u^2 + p)_x = 0, \\ (\rho v)_t + (\rho uv)_x = 0 \end{cases} \tag{1.1}$$

consisting of three scalar equations, namely, the conservation of mass and two linear momentums, in which $\rho > 0$ and (u, v) represent the density and velocity of the fluid, respectively, $p = p(\rho)$ stands for the scalar pressure.

System (1.1) is indeed a reduced model of the two-dimensional isentropic compressible Euler system [32]

$$\begin{cases} \rho_t + (\rho u)_x + (\rho v)_y = 0, \\ (\rho u)_t + (\rho u^2 + p)_x + (\rho uv)_y = 0, \\ (\rho v)_t + (\rho uv)_x + (\rho v^2 + p)_y = 0. \end{cases} \tag{1.2}$$

The main motivation for considering the one-dimensional simplified model (1.1) lies in that the Cauchy problem for the two-dimensional isentropic compressible Euler system (1.2) remains formidable for its complexity, even for the Riemann problem, which is the simplest Cauchy problem. What is more, the reduced model (1.1) is also encountered such as in [10, 14] when the solutions (ρ, u, v) with the claimed properties that are independent of y-variable.

In order to analyze the phenomena of concentration and cavitation in solutions, in this paper, the state equation for (1.1) is considered as the generalized Chaplygin gas (GCG)

$$p(\rho) = -\frac{\epsilon}{\rho^\alpha}, \tag{1.3}$$

which reflects the relation between pressure p and density ρ, where $0 < \alpha < 1$ is constant, $\epsilon > 0$ is a small scaling perturbed parameter modeling the strength of pressure p. The GCG (1.3) with the negative pressure and positive sound speed was proposed in [1], where its relation to a scalar-field Lagrangian of a generalized Born-Infeld type was clarified. In present, the cosmological models based on the dynamics of generalized Chaplygin gases have attracted considerable interest [2, 22]. Specially, when $\alpha = 1$, (1.3) is called the Chaplygin gas (CG), which is connected to string theory and was initially introduced by Chaplygin [7], Tsien [27], and von Karman [28] as a suitable mathematical approximation to compute the lifting force on an airplane wing in aerodynamics. Currently, the CG and GCG are regarded as the possible phenomenological models for dark energy and used to describe the accelerating expansion of the universe.

It should be claimed that, although the parameter ϵ in (1.3) can be considered very small and reflects the strength of the underlying pressure, it does not vanish in general. We propose to include this parameter in hopes of understanding the process of the formation of concentration and cavitation in the isentropic compressible Euler equations (1.1). Particularly, as $\epsilon \to 0$, that is, the pressure vanishes, the system (1.1) formally becomes the pressureless gas dynamics (PGD) model

$$\begin{cases} \rho_t + (\rho u)_x = 0, \\ (\rho u)_t + (\rho u^2)_x = 0, \\ (\rho v)_t + (\rho uv)_x = 0, \end{cases} \tag{1.4}$$

which is also called the zero-pressure flow model or constant pressure fluid dynamics. The system of zero-pressure type fluid dynamics is usually used to describe some important physical phenomena, such as the motion of free particles sticking together under collision [3] and the formation of large scale structures in the universe [12, 23].

The Riemann problem for (1.4) with piecewise constant initial data

$$(\rho, u, v)(0, x) = \begin{cases} (\rho_-, u_-, v_-), & x < 0, \\ (\rho_+, u_+, v_+), & x > 0 \end{cases} \tag{1.5}$$

has been studied by Hu [14], where $\rho_\pm > 0$, $u_\pm$ and $v_\pm$ are constants. The Riemann solution has been constructed by virtue of the viscosity vanishing approach. Interestingly, a special type of nonlinear singular shock wave called the delta shock wave is found in solution. Meanwhile, the vacuum state also appears. Since the three eigenvalues of the zero-pressure flow (1.4) coincide, the occurrence of delta shock waves and vacuum states as $t > 0$ may be regarded as a result of resonance among the three characteristic fields. Besides, one can refer to [34] for the interactions of delta shock waves and vacuum states for (1.4).

Mathematically, the delta shock wave and vacuum state are used to describe the phenomena of concentration and cavitation, respectively. A delta shock wave is a new kind of discontinuity, on which at least one of the state variables may develop an extreme concentration in the form of a weighted Dirac delta function with the discontinuity as its support. It is more compressive than a traditional shock wave in the sense that more characteristics will enter the discontinuity line. Nowadays, the delta shock wave has become a hot topic in the study of hyperbolic conservation laws. Besides, it is worth recalling that, although the delta shock wave is also obtained in solutions of (1.1) and (1.2) for CG (see [13, 26]), the occurrence mechanism of which is essentially different from that of the PGD model (1.4). For the former, the system is strict hyperbolic and owns three kinds of degenerated characteristics. While for the later, the system has three repeated degenerated characteristics and as a result the strict hyperbolicity fails.

In order to rigorously justify the formation of concentration and cavitation as well as the appearance of delta shock wave and vacuum state, an effective approach is the so called vanishing pressure limit method. This method may date back to the beginning of 21st century when Li [17] and Chen and Liu [8, 9] studied the asymptotic behavior of solutions to the compressible Euler equations by means of imposing the pressure or temperature drop to zero. Since then, by using this method, a large number of scholars have investigated the formation mechanism of delta shocks and vacuums in various conservation laws and achieved a series of fruitful results, which makes the researches on this subject particularly noticeable.

As for the vanishing pressure limit of solutions to CG and GCG equations, some literatures have been contributed. For example, Sheng et al. [25] studied the vanishing pressure limit of solutions to the isentropic Euler equations for generalized Chaplygin gas; Zhang et al. [33] analyzed the concentration and cavitation in the vanishing pressure limit of solutions to the generalized Chaplygin Euler equations of compressible fluid flow. See also Pan and Han [19] for the Aw-Rascle traffic flow model with CG equation, Yin and Song [30] as well as Li and Shao [16] for the CG and GCG for relativistic fluid, etc. Recently, the authors in [11, 18] discussed the vanishing pressure limit of Riemann solutions to the non-isentropic Euler equations for CG and GCG, respectively. Besides, the vanishing pressure limit of solutions to (1.1) with polytropic gas was studied by Zhang [31].

Motivated by the above discussions, we in this paper focus on the phenomena of concentration and cavitation as well as the limit behavior of solutions to the GCG equations (1.1), (1.3) in vanishing pressure. It is shown that, when ϵ decreases to a certain critical value, any Riemann solution of (1.1), (1.3) containing two shocks and possibly one-contact-discontinuity converges to a delta-shock solution of the system itself. Moreover, as $\epsilon \to 0$, the limiting solution is nothing but the delta-shock solution of the PGD model (1.4), and the intermediate density between the two shocks tends to an extreme concentration in the form of a weighted δ-measure that forms the delta shock wave. By contrast, any Riemann solution of (1.1), (1.3) containing two rarefaction waves and possibly one contact-discontinuity tends to a two-contact-discontinuity solution of PGD model (1.4), and the nonvacuum intermediate state in between tends to a vacuum state. These indicate a physical fact in fluid dynamics, that is, as the limit of solution in vanishing pressure, a delta shock wave for the PGD model (1.4) is a result of concentration of density, while a vacuum state is a result of cavitation. It is noticed that, our result is similar to that of Shen and Sun [24], in which the formation of delta shock wave and vacuum state for a 3×3 two-phase flow model was systemically studied.

Finally, by the second-order non-oscillatory central schemes [15], we examine the formation processes of delta shock waves and vacuum states with some numerical results as ϵ decreases. The numerical simulations are completely coinciding with the theoretical analysis.

This paper is organized as follows. Section 2 restates the Riemann solutions to the PGD model (1.4). In Section 3, we solve the Riemann problem (1.5) for the GCG equations (1.1), (1.3), and discuss the dependence of solutions on the parameter ϵ. In Sections 4 and 5, we investigate the limits of solutions to (1.1), (1.3). Section 6 exhibits some numerical results.

2. Delta shocks and vacuums for the PGD model (1.4)

We will begin with reviewing delta shock waves and vacuum states of (1.4), (1.5). Readers can refer to [14, 31] for more details.

The system (1.4) has a triple eigenvalue $\lambda = u$ and two right eigenvectors $\overrightarrow{r_1} = (1, 0, 0)^T$,

$\overrightarrow{r_2} = (0,0,1)^T$. From $\nabla\lambda \cdot \overrightarrow{r_i} \equiv 0$ $(i = 1,2)$, we know that the characteristic λ is linearly degenerate. Thus, the elementary waves involve only contact discontinuities.

Noting that (1.4) and (1.5) are invariant under the uniform stretching of coordinates: $(t,x) \to (\beta t, \beta x)$ (β is constant), it follows that if the solution is unique, then the solution must depend on x/t alone. Thus, we look for the self-similar solutions of (1.4) and (1.5) as follows

$$(\rho,u,v)(t,x) = (\rho,u,v)(\xi), \quad \xi = x/t. \tag{2.1}$$

Then, the Riemann problem (1.4) and (1.5) is reduced to the boundary value problem

$$-\xi\rho_\xi + (\rho u)_\xi = 0, \quad -\xi(\rho u)_\xi + (\rho u^2)_\xi = 0, \quad -\xi(\rho v)_\xi + (\rho uv)_\xi = 0 \tag{2.2}$$

with the boundary condition $(\rho,u,v)(\pm\infty) = (\rho_\pm, u_\pm, v_\pm)$.

As in [14, 31], the solution of (1.4), (1.5) can be constructed by two cases.

When $u_- < u_+$, the solution containing two contact discontinuities and a vacuum state can be shown as

$$(\rho,u,v)(\xi) = \begin{cases} (\rho_-,u_-,v_-), & -\infty < \xi < u_-, \\ (0,u(\xi),v(\xi)), & u_- \le \xi \le u_+, \\ (\rho_+,u_+,v_+), & u_+ < \xi < +\infty, \end{cases} \tag{2.3}$$

in which $u(\xi)$ and $v(\xi)$ are two smooth functions.

When $u_- > u_+$, one needs to introduce the delta-shock solution since the singularity of solution must develop due to the overlap of characteristic lines. For this purpose, the definition of a weighted delta function supported on a curve is given at first.

Definition 2.1. A two-dimensional weighted delta function $w(s)\delta_S$ supported on a smooth curve S parameterized as $t = t(s)$, $x = x(s)$ $(a \le s \le b)$ is defined by

$$\big\langle w(t(s))\delta_S, \phi(t(s),x(s))\big\rangle = \int_a^b w(t(s))\phi(t(s),x(s))\sqrt{x'(s)^2 + t'(s)^2}ds \tag{2.4}$$

for all test functions $\phi(t,x) \in C_0^\infty(R^+ \times R^1)$.

Based on this definition, we can introduce a family of delta-shock solutions with the parameter σ to construct the solution of (1.4), which takes the form

$$\rho(t,x) = \rho_0(t,x) + w(t)\delta_S, \quad u(t,x) = u_0(t,x), \quad v(t,x) = v_0(t,x), \tag{2.5}$$

where $S = \{(t,\sigma t) : 0 \le t < \infty\}$, and

$$\begin{cases} \rho_0(t,x) = \rho_- + [\rho]\chi(x-\sigma t), & u_0(t,x) = u_- + [u]\chi(x-\sigma t), \\ v_0(t,x) = v_- + [v]\chi(x-\sigma t), & w(t) = \dfrac{t}{\sqrt{1+\sigma^2}}(\sigma[\rho] - [\rho u]), \end{cases} \tag{2.6}$$

where $[h] = h_+ - h_-$ is the jump of h, σ the velocity of the delta shock wave, and $\chi(x)$ the characteristic function that is 0 when $x < 0$ and 1 when $x > 0$.

Moreover, the the delta-shock solution of (1.4) constructed above satisfies

$$\langle \rho, \phi_t\rangle + \langle \rho u, \phi_x\rangle = 0, \quad \langle \rho u, \phi_t\rangle + \langle \rho u^2, \phi_x\rangle = 0, \quad \langle \rho v, \phi_t\rangle + \langle \rho uv, \phi_x\rangle = 0 \tag{2.7}$$

for all test functions $\phi \in C_0^\infty(R^+ \times R^1)$, where

$$\langle \rho, \phi\rangle = \int_0^{+\infty}\int_{-\infty}^{+\infty} \rho_0 \phi dxdt + \langle w\delta_S, \phi\rangle, \quad \langle \rho u, \phi\rangle = \int_0^{+\infty}\int_{-\infty}^{+\infty} \rho_0 u_0 \phi dxdt + \langle \sigma w\delta_S, \phi\rangle,$$

and v has the similar integral identities as above.

Then, we look for a piecewise smooth solution to (1.4) in the form

$$(\rho, u, v)(t,x) = \begin{cases} (\rho_-, u_-, v_-), & x < x(t), \\ \big(w(t)\delta(x - x(t)), u_\delta, v_\delta\big), & x = x(t), \\ (\rho_+, u_+, v_+), & x > x(t), \end{cases} \tag{2.8}$$

where $w(t)$ is the strength of the delta shock wave, and u_δ, v_δ are the corresponding values of u and v on the discontinuous curve $x = x(t)$.

The solution (2.8) should obey the generalized Rankine-Hugoniot relation

$$\begin{cases} \dfrac{dx}{dt} = \sigma_0 = u_\delta, \\ \dfrac{d\big(w(t)\sqrt{1+\sigma_0^2}\big)}{dt} = [\rho]u_\delta - [\rho u], \\ \dfrac{d\big(w(t)u_\delta\sqrt{1+\sigma_0^2}\big)}{dt} = [\rho u]u_\delta - [\rho u^2], \\ \dfrac{d\big(w(t)v_\delta\sqrt{1+\sigma_0^2}\big)}{dt} = [\rho v]u_\delta - [\rho uv] \end{cases} \tag{2.9}$$

and the entropy condition

$$u_+ < \sigma_0 < u_-. \tag{2.10}$$

Here, we use $\frac{dx}{dt} = \sigma_0 = u_\delta$ to denote the propagation speed of delta shock wave for the reason that the concentration of ρ needs to travel at the same propagation speed of the discontinuity.

Solving the generalized Rankine-Hugoniot relation (2.9) under the entropy condition (2.10) with the initial data $x(0) = 0$ and $w(0) = 0$ yields that

$$\sigma_0 = u_\delta = \frac{\sqrt{\rho_-}u_- + \sqrt{\rho_+}u_+}{\sqrt{\rho_-} + \sqrt{\rho_+}}, \quad v_\delta = \frac{\sqrt{\rho_-}v_- + \sqrt{\rho_+}v_+}{\sqrt{\rho_-} + \sqrt{\rho_+}}, \quad w(t) = \frac{\sqrt{\rho_-\rho_+}(u_- - u_+)}{\sqrt{1+\sigma_0^2}}t \tag{2.11}$$

for $\rho_- \neq \rho_+$, and

$$\sigma_0 = u_\delta = \frac{u_- + u_+}{2}, \quad v_\delta = \frac{v_- + v_+}{2}, \quad w(t) = \frac{\rho_- u_- - \rho_+ u_+}{\sqrt{1+\sigma_0^2}}t \tag{2.12}$$

for $\rho_- = \rho_+$, which is just the delta-shock solution of (1.4) defined by (2.5) and (2.6).

3. Riemann solution to the GCG equations (1.1) and (1.3)

In this section, we put the Riemann problem (1.1) and (1.3) with (1.5).

3.1. Solution involving classical waves

The eigenvalues for system (1.1) are

$$\lambda_1^\epsilon = u - \sqrt{\epsilon\alpha}\rho^{-\frac{1+\alpha}{2}}, \quad \lambda_2^\epsilon = u, \quad \lambda_3^\epsilon = u + \sqrt{\epsilon\alpha}\rho^{-\frac{1+\alpha}{2}}, \tag{3.1}$$

with the associated right eigenvectors

$$\overrightarrow{r}_1^\epsilon = \left(\rho, -\sqrt{\epsilon\alpha}\rho^{-\frac{1+\alpha}{2}}, 0\right)^T, \quad \overrightarrow{r}_2^\epsilon = (0,0,1)^T, \quad \overrightarrow{r}_3^\epsilon = \left(\rho, \sqrt{\epsilon\alpha}\rho^{-\frac{1+\alpha}{2}}, 0\right)^T, \tag{3.2}$$

respectively. Clearly, (1.1) is strictly hyperbolic. Denoted by $\nabla = (\partial_\rho, \partial_u, \partial_v)$, then for $0 < \alpha < 1$, one can check that

$$\nabla\lambda_1^\epsilon \cdot \overrightarrow{r}_1^\epsilon = \frac{\alpha-1}{2}\sqrt{\epsilon\alpha}\rho^{-\frac{1+\alpha}{2}} < 0, \quad \nabla\lambda_2^\epsilon \cdot \overrightarrow{r}_2^\epsilon = 0, \quad \nabla\lambda_3^\epsilon \cdot \overrightarrow{r}_3^\epsilon = \frac{1-\alpha}{2}\sqrt{\epsilon\alpha}\rho^{-\frac{1+\alpha}{2}} > 0.$$

So, λ_1^ϵ and λ_3^ϵ are genuinely nonlinear for $\rho > 0$ and λ_2^ϵ is always linearly degenerate.

As in Section 2, we look for the self-similar solution $(\rho,u,v)(t,x) = (\rho,u,v)(\xi)$ ($\xi = x/t$), then the Riemann problem (1.1) and (1.5) changes into the boundary value problem

$$-\xi\rho_\xi + (\rho u)_\xi = 0, \quad -\xi(\rho u)_\xi + \left(\rho u^2 - \frac{\epsilon}{\rho^\alpha}\right)_\xi = 0, \quad -\xi(\rho v)_\xi + (\rho uv)_\xi = 0 \tag{3.3}$$

with $(\rho,u,v)(\pm\infty) = (\rho_\pm, u_\pm, v_\pm)$.

For smooth solution, (3.3) can be rewritten as

$$\begin{pmatrix} u-\xi & \rho & 0 \\ \epsilon\alpha\rho^{-(1+\alpha)} & \rho(u-\xi) & 0 \\ 0 & 0 & \rho(u-\xi) \end{pmatrix} \begin{pmatrix} \rho \\ u \\ v \end{pmatrix}_\xi = 0, \tag{3.4}$$

which provides either the general constant solution $(\rho,u,v) = Const.$, or the backward centered rarefaction wave

$$\overleftarrow{R}: \ \xi = u - \sqrt{\epsilon\alpha}\rho^{-\frac{1+\alpha}{2}}, \quad \frac{du}{d\rho} = -\sqrt{\epsilon\alpha}\rho^{-\frac{1+\alpha}{2}-1}, \quad dv = 0, \tag{3.5}$$

or the forward centered rarefaction wave

$$\overrightarrow{R}: \ \xi = u + \sqrt{\epsilon\alpha}\rho^{-\frac{1+\alpha}{2}}, \quad \frac{du}{d\rho} = \sqrt{\epsilon\alpha}\rho^{-\frac{1+\alpha}{2}-1}, \quad dv = 0. \tag{3.6}$$

For a given left state (ρ_-, u_-, v_-), the possible states (ρ,u,v) that can be connected to (ρ_-, u_-, v_-) by a backward or forward centered rarefaction wave are symbolized by $\overleftarrow{R}(\rho_-, u_-, v_-)$ or $\overrightarrow{R}(\rho_-, u_-, v_-)$. Then, under the requirement $\lambda_1^\epsilon(\rho_-, u_-, v_-) < \lambda_1^\epsilon(\rho,u,v)$, we integrate (3.5) to obtain the backward centered rarefaction wave

$$\overleftarrow{R}(\rho_-, u_-, v_-): \begin{cases} \xi = \lambda_1^\epsilon = u - \sqrt{\epsilon\alpha}\rho^{-\frac{1+\alpha}{2}}, \\ u - \dfrac{2\sqrt{\epsilon\alpha}}{1+\alpha}\rho^{-\frac{1+\alpha}{2}} = u_- - \dfrac{2\sqrt{\epsilon\alpha}}{1+\alpha}\rho_-^{-\frac{1+\alpha}{2}}, \quad \rho < \rho_-, \\ v = v_-. \end{cases} \tag{3.7}$$

Similarly, the forward centered rarefaction wave

$$\overrightarrow{R}(\rho_-, u_-, v_-): \begin{cases} \xi = \lambda_3^\epsilon = u + \sqrt{\epsilon\alpha}\rho^{-\frac{1+\alpha}{2}}, \\ u + \dfrac{2\sqrt{\epsilon\alpha}}{1+\alpha}\rho^{-\frac{1+\alpha}{2}} = u_- + \dfrac{2\sqrt{\epsilon\alpha}}{1+\alpha}\rho_-^{-\frac{1+\alpha}{2}}, \quad \rho > \rho_-, \\ v = v_- \end{cases} \tag{3.8}$$

is derived by integrating (3.6) with the requirement $\lambda_3^\epsilon(\rho_+, u_+, v_+) > \lambda_3^\epsilon(\rho, u, v)$.

Analogously, for a given state (ρ_+, u_+, v_+), we can obtain $\overleftarrow{R}(\rho_+, u_+, v_+)$ or $\overrightarrow{R}(\rho_+, u_+, v_+)$.

For the bounded discontinuity at $\xi = \omega^\epsilon$, it obeys the Rankine-Hugoniot condition

$$\begin{cases} \omega^\epsilon[\rho] = [\rho u], \\ \omega^\epsilon[\rho u] = \left[\rho u^2 - \dfrac{\epsilon}{\rho^\alpha}\right], \\ \omega^\epsilon[\rho v] = [\rho u v], \end{cases} \tag{3.9}$$

from which we have either a backward shock wave

$$\overleftarrow{S}: \ \omega_1^\epsilon = u_- - \sqrt{\frac{\rho_+[-\epsilon\rho^{-\alpha}]}{\rho_-[\rho]}}, \quad u_+ = u_- - \sqrt{\frac{[-\epsilon\rho^{-\alpha}]}{\rho_+\rho_-[\rho]}}(\rho_+ - \rho_-), \quad v_+ = v_-, \tag{3.10}$$

a contact discontinuity

$$J: \ \omega_2^\epsilon = u_- = u_+, \quad \rho_- = \rho_+, \quad u_- = u_+, \quad , v_- \neq v_+, \tag{3.11}$$

or a forward shock wave

$$\overrightarrow{S}: \ \omega_3^\epsilon = u_- + \sqrt{\frac{\rho_+[-\epsilon\rho^{-\alpha}]}{\rho_-[\rho]}}, \quad u_+ = u_- - \sqrt{\frac{[-\epsilon\rho^{-\alpha}]}{\rho_+\rho_-[\rho]}}(\rho_- - \rho_+), \quad v_+ = v_-. \tag{3.12}$$

Similar to the rarefaction waves, for a given state (ρ_-, u_-, v_-), the possible states (ρ, u, v) that can be connected to (ρ_-, u_-, v_-) by a backward or forward shock wave are symbolized by $\overleftarrow{S}(\rho_-, u_-, v_-)$ or $\overrightarrow{S}(\rho_-, u_-, v_-)$. Then, by (3.10) and the Lax shock inequalities $\lambda_1^\epsilon(\rho, u, v) < \omega_1^\epsilon < \lambda_1^\epsilon(\rho_-, u_-, v_-)$ and $\omega_1^\epsilon < \lambda_2^\epsilon(\rho, u, v)$, we obtain the backward shock wave

$$\overleftarrow{S}(\rho_-, u_-, v_-): \begin{cases} \omega_1^\epsilon = u_- - \sqrt{\dfrac{\epsilon\rho}{\rho_-(\rho - \rho_-)} \cdot \left(\dfrac{1}{\rho_-^\alpha} - \dfrac{1}{\rho^\alpha}\right)}, \\ u = u_- - \sqrt{\epsilon\left(\dfrac{1}{\rho_-} - \dfrac{1}{\rho}\right)\left(\dfrac{1}{\rho_-^\alpha} - \dfrac{1}{\rho^\alpha}\right)}, \quad \rho > \rho_-, \\ v = v_-. \end{cases} \tag{3.13}$$

Using (3.11), we get the contact discontinuity curve

$$J(\rho_-, u_-, v_-): \ \omega_2^\epsilon = u, \quad \rho = \rho_-, \quad u = u_-, \quad v_+ \neq v_-, \tag{3.14}$$

which is the set of states that can be joined with the left state (ρ_-, u_-, v_-) by a contact discontinuity. Analogously, using (3.12) and the Lax shock inequalities $\lambda_3^\epsilon(\rho, u, v) < \omega_3^\epsilon <$

$\lambda_3^\epsilon(\rho_-,u_-,v_-)$ and $\omega_3^\epsilon>\lambda_2^\epsilon(\rho_-,u_-,v_-)$, we obtain the forward shock wave curve

$$\overrightarrow{S}(\rho_-,u_-,v_-):\begin{cases}\omega_3^\epsilon=u_-+\sqrt{\dfrac{\epsilon\rho}{\rho_-(\rho-\rho_-)}\cdot\left(\dfrac{1}{\rho_-^\alpha}-\dfrac{1}{\rho^\alpha}\right)},\\ u=u_--\sqrt{\epsilon\left(\dfrac{1}{\rho_-}-\dfrac{1}{\rho}\right)\left(\dfrac{1}{\rho_-^\alpha}-\dfrac{1}{\rho^\alpha}\right)},\quad \rho<\rho_-,\\ v=v_-.\end{cases}\tag{3.15}$$

Similarly, for a given state (ρ_+,u_+,v_+), we can obtain $\overleftarrow{S}(\rho_+,u_+,v_+)$ or $\overrightarrow{S}(\rho_+,u_+,v_+)$.

Obviously, the classical waves of system (1.1) and (1.3) contain a centered rarefaction wave, a shock wave, and a contact discontinuity.

In what follows, let us construct the Riemann solution for (1.1) and (1.3). Noting that the state variables ρ and u are invariant and only the state variable v varies when across J, the slip line. Thus, motivated by [20, 21, 26], we are able to consider the elementary wave curves projected onto the upper-half (u,ρ)-phase plane. Here, the positions of ρ and u are exchanged in the phase plane just for convenience. The benefit of considering such a projection plane is that we can solve the 3×3 GCG equations (1.1) and (1.3) by analogy with the relevant methods of solving the 2×2 isentropic GCG equations.

For the fixed left state (ρ_-,u_-,v_-), denoted by $\overleftarrow{R}(\rho_-,u_-)$, $\overrightarrow{R}(\rho_-,u_-)$, $\overleftarrow{S}(\rho_-,u_-)$ and $\overrightarrow{S}(\rho_-,u_-)$ the projection curves of the classical wave curves (3.7), (3.8), (3.13) and (3.15) in the (u,ρ)-phase plane, respectively. Then, by a similar analysis as in [25, 26, 29], we know that $\frac{du}{d\rho}<0$ for $\overleftarrow{R}(\rho_-,u_-)$ and $\overleftarrow{S}(\rho_-,u_-)$, while $\frac{du}{d\rho}>0$ for $\overrightarrow{R}(\rho_-,u_-)$ and $\overrightarrow{S}(\rho_-,u_-)$. Moreover, $\overleftarrow{S}(\rho_-,u_-)$ has the asymptote $u=u_--\sqrt{\epsilon}\rho_-^{-\frac{1+\alpha}{2}}$, $\overrightarrow{S}(\rho_+,u_+)$ has the asymptote $u=u_++\sqrt{\epsilon}\rho_+^{-\frac{1+\alpha}{2}}$, and $\overrightarrow{R}(\rho_-,u_-)$ has its asymptote $u=u_-+\frac{2\sqrt{\epsilon\alpha}}{1+\alpha}\rho_-^{-\frac{1+\alpha}{2}}$.

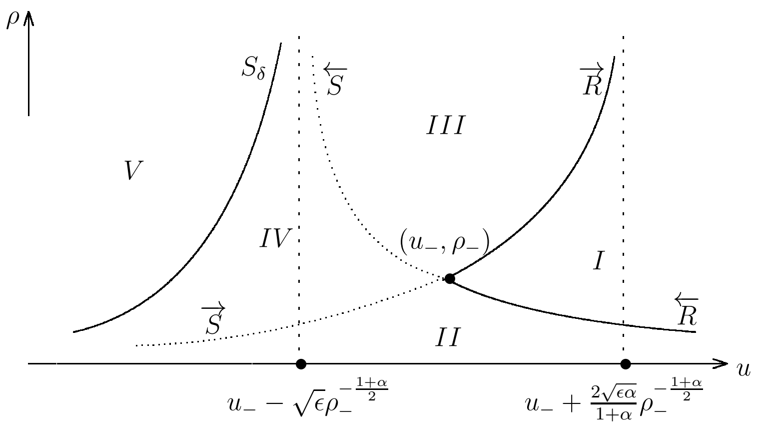

Fig.3.1. The projections of wave curves for (1.1) and (1.3) onto (u,ρ) plane.

In addition, as done in [25, 26, 29], we draw a curve S_δ as follows

$$S_\delta:\ u+\sqrt{\epsilon}\rho^{-\frac{1+\alpha}{2}}=u_--\sqrt{\epsilon}\rho_-^{-\frac{1+\alpha}{2}},\quad \rho>0,\tag{3.16}$$

which is indeed the projection of the boundary for the region where nonclassical solutions appear. Then, the upper-half (u,ρ)-phase plane is divided into five regions I,II,III,IV and V, as shown in Fig.3.1.

By the analysis method in phase plane, we construct the solution of (1.1) and (1.3). When the projection of (ρ_+, u_+, v_+) onto (u, ρ)-phase plane $(\rho_+, u_+) \in I \cup II \cup III \cup IV$, namely, $u_- - \sqrt{\epsilon}\rho_-^{-\frac{1+\alpha}{2}} < u_+ + \sqrt{\epsilon}\rho_+^{-\frac{1+\alpha}{2}}$, the Riemann solution to (1.1) and (1.3) can be expressed in the following form:

(1). $(\rho_+, u_+) \in I : (\rho_-, u_-, v_-) + \overleftarrow{R} + (\rho_*, u_*, v_{*1}) + J + (\rho_*, u_*, v_{*2}) + \overrightarrow{R} + (\rho_+, u_+, v_+)$;

(2). $(\rho_+, u_+) \in II : (\rho_-, u_-, v_-) + \overleftarrow{R} + (\rho_*, u_*, v_{*1}) + J + (\rho_*, u_*, v_{*2}) + \overrightarrow{S} + (\rho_+, u_+, v_+)$;

(3). $(\rho_+, u_+) \in III : (\rho_-, u_-, v_-) + \overleftarrow{S} + (\rho_*, u_*, v_{*1}) + J + (\rho_*, u_*, v_{*2}) + \overrightarrow{R} + (\rho_+, u_+, v_+)$;

(4). $(\rho_+, u_+) \in IV : (\rho_-, u_-, v_-) + \overleftarrow{S} + (\rho_*, u_*, v_{*1}) + J + (\rho_*, u_*, v_{*2}) + \overrightarrow{S} + (\rho_+, u_+, v_+)$,

where (ρ_*, u_*, v_{*1}) and (ρ_*, u_*, v_{*2}) are the intermediate states satisfying $v_{*1} = v_-$, $v_{*2} = v_+$.

Theorem 3.1. Under the condition $u_- - \sqrt{\epsilon}\rho_-^{-\frac{1+\alpha}{2}} < u_+ + \sqrt{\epsilon}\rho_+^{-\frac{1+\alpha}{2}}$, the Riemann solution to (1.1) and (1.3) admits four kinds of different configurations, which consist of a centered rarefaction wave, a shock wave, and a contact discontinuity besides the constant states.

Remark 3.1. For the CG ($\alpha = 1$), the characteristic fields of (1.1) and (1.3) are linearly degenerate, so all of the rarefaction waves and shock waves become the contact discontinuities.

3.2. Delta shock wave solution

When the projection of (ρ_+, u_+, v_+) onto (u, ρ)-phase plane $(\rho_+, u_+) \in V$, namely, $u_+ + \sqrt{\epsilon}\rho_+^{-\frac{1+\alpha}{2}} < u_- - \sqrt{\epsilon}\rho_-^{-\frac{1+\alpha}{2}}$, we need to seek a nonclassical solution. In fact, from the above discussions, we know that the nonclassical solution may occur under the condition that $u_+ + \sqrt{\epsilon}\rho_+^{-\frac{1+\alpha}{2}} \leq u_- - \sqrt{\epsilon}\rho_-^{-\frac{1+\alpha}{2}}$. In this situation, we have

$$\lambda_1^\epsilon(+) < \lambda_2^\epsilon(+) < \lambda_3^\epsilon(+) \leq \lambda_1^\epsilon(-) < \lambda_2^\epsilon(-) < \lambda_3^\epsilon(-),$$

where $(\pm) = (\rho_\pm, u_\pm, v_\pm)$, namely,

$$u_+ - \sqrt{\epsilon\alpha}\rho_+^{-\frac{1+\alpha}{2}} < u_+ < u_+ + \sqrt{\epsilon\alpha}\rho_+^{-\frac{1+\alpha}{2}} \leq u_- - \sqrt{\epsilon\alpha}\rho_-^{-\frac{1+\alpha}{2}} < u_- < u_- + \sqrt{\epsilon\alpha}\rho_-^{-\frac{1+\alpha}{2}},$$

which means that the characteristic lines from initial data will overlap in the domain Ω, as shown in Fig.3.2. So singularity must happen in Ω. It is well known that the singularity is impossible to be a jump with finite amplitude, which implies that there is no solution that is piecewise smooth and bounded.

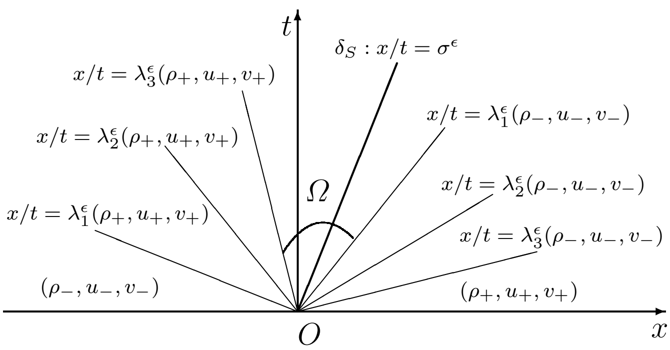

Fig.3.2. Analysis of characteristics for delta-shock of (1.1) and (1.3).

Motivated by [20, 21, 25, 26, 29], etc., the solution for (1.1) with delta distribution at the jump (i.e., the delta-shock solution) should be constructed, which is, under the Definition 2.1,

$$\rho(t,x) = \rho_0(t,x) + w^\epsilon(t)\delta_S, \quad u(t,x) = u_0(t,x), \quad v(t,x) = v_0(t,x), \tag{3.17}$$

where $S = \{(t, \sigma^\epsilon t) : 0 \le t < \infty\}$, and

$$\begin{cases} \rho_0(t,x) = \rho_- + [\rho]\chi(x - \sigma^\epsilon t), \quad u_0(t,x) = u_- + [u]\chi(x - \sigma^\epsilon t), \\ v_0(t,x) = v_- + [v]\chi(x - \sigma^\epsilon t), \quad w^\epsilon(t) = \dfrac{t}{\sqrt{1+(\sigma^\epsilon)^2}}(\sigma^\epsilon[\rho] - [\rho u]), \end{cases} \tag{3.18}$$

where $\frac{1}{\rho^\alpha}$ is defined as [25, 29]

$$\frac{1}{\rho^\alpha} = \begin{cases} \dfrac{1}{\rho_-^\alpha}, & x < \sigma^\epsilon t, \\ 0, & x = \sigma^\epsilon t, \\ \dfrac{1}{\rho_+^\alpha}, & x > \sigma^\epsilon t. \end{cases} \tag{3.19}$$

As before, we seek a delta shock wave solution with the discontinuity $x = x^\epsilon(t)$ to (1.1) and (1.3) in the form

$$(\rho, u, v)(t,x) = \begin{cases} (\rho_-, u_-, v_-), & x < x^\epsilon(t), \\ \big(w^\epsilon(t)\delta(x - x^\epsilon(t)), u_\delta^\epsilon, v_\delta^\epsilon\big), & x = x^\epsilon(t), \\ (\rho_+, u_+, v_+), & x > x^\epsilon(t), \end{cases} \tag{3.20}$$

where $w^\epsilon(t)$ is the strength of the delta shock wave, and $u_\delta^\epsilon, v_\delta^\epsilon$ are the corresponding values of u and v on the discontinuous curve $x = x^\epsilon(t)$.

Lemma 3.2. The delta-shock solution of the form (3.20) should satisfy the following generalized Rankine-Hugoniot condition

$$\begin{cases} \dfrac{dx^\epsilon(t)}{dt} = \sigma^\epsilon = u_\delta^\epsilon, \\ \dfrac{d\big(w^\epsilon(t)\sqrt{1+(\sigma^\epsilon)^2}\big)}{dt} = [\rho]u_\delta^\epsilon - [\rho u], \\ \dfrac{d\big(w^\epsilon(t)u_\delta^\epsilon\sqrt{1+(\sigma^\epsilon)^2}\big)}{dt} = [\rho u]u_\delta^\epsilon - \left[\rho u^2 - \dfrac{\epsilon}{\rho^\alpha}\right], \\ \dfrac{d\big(w^\epsilon(t)v_\delta^\epsilon\sqrt{1+(\sigma^\epsilon)^2}\big)}{dt} = [\rho v]u_\delta^\epsilon - [\rho uv]. \end{cases} \tag{3.21}$$

Proof. We only prove the third one of (3.21). As a matter of fact, for any test function $\phi \in C_0^\infty(R^+ \times R^1)$, using the previous symbols in (2.7), we have

$$\begin{aligned} I_3 &= \langle \rho^\epsilon u^\epsilon, \phi_t \rangle + \left\langle \rho^\epsilon (u^\epsilon)^2 - \frac{\epsilon}{(\rho^\epsilon)^\alpha}, \phi_x \right\rangle \\ &= \int_0^{+\infty}\int_{-\infty}^{+\infty} \left(\rho^\epsilon u^\epsilon \phi_t + \left(\rho^\epsilon (u^\epsilon)^2 - \frac{\epsilon}{(\rho^\epsilon)^\alpha} \right) \phi_x \right) dxdt \\ &\quad + \int_0^{+\infty} \Big(w^\epsilon(t)\sigma^\epsilon \sqrt{1+(\sigma^\epsilon)^2}\phi_t + w^\epsilon(t)(\sigma^\epsilon)^2 \sqrt{1+(\sigma^\epsilon)^2}\phi_x \Big) dt. \end{aligned}$$

Then, I_3 can be composed as

$$I_3 = \int_0^{+\infty}\int_{-\infty}^{x(t)} \Big((\rho_- u_-\phi)_t + \Big(\rho_- u_-^2 - \frac{\epsilon}{\rho_-^\alpha}\phi\Big)_x\Big) dxdt$$

$$+\int_0^{+\infty}\int_{x(t)}^{+\infty} \Big((\rho_+ u_+\phi)_t + \Big(\rho_+ u_+^2 - \frac{\epsilon}{\rho_+^\alpha}\phi\Big)_x\Big) dxdt + \int_0^{+\infty} w^\epsilon(t)\sigma^\epsilon\sqrt{1+(\sigma^\epsilon)^2}(\phi_t + \sigma^\epsilon\phi_x)dt.$$

By Green's formulation and integrating by parts, we have

$$\begin{aligned} I_3 &= -\int_0^{+\infty} -\left(\rho_- u_-^2 - \frac{\epsilon}{\rho_-^\alpha}\right)\phi dt + \rho_- u_-\phi dx \\ &\quad + \int_0^{+\infty} -\left(\rho_+ u_+^2 - \frac{\epsilon}{\rho_+^\alpha}\right)\phi dt + \rho_+ u_+\phi dx - \int_0^{+\infty}\frac{d\big(w^\epsilon(t)\sigma^\epsilon\sqrt{1+(\sigma^\epsilon)^2}\big)}{dt}\phi dt \\ &= \int_0^{+\infty}\left([\rho u]u_\delta^\epsilon - \left[\rho u^2 - \frac{\epsilon}{\rho^\alpha}\right] - \frac{d\big(w^\epsilon(t)u_\delta^\epsilon\sqrt{1+(\sigma^\epsilon)^2}\big)}{dt}\right)\phi dt. \end{aligned}$$

Thus, the third equation of (3.21) is obtained by taking $I_3 = 0$. The second and last equations can be proved similarly. This is the end of the proof. □

To guarantee the uniqueness, the delta-shock solution must obey the entropy condition

$$u_+ + \sqrt{\epsilon\alpha}\rho_+^{-\frac{1+\alpha}{2}} < \sigma^\epsilon = u_\delta^\epsilon < u_- - \sqrt{\epsilon\alpha}\rho_-^{-\frac{1+\alpha}{2}}, \tag{3.22}$$

which means that all of the six characteristic lines on both sides of the discontinuity are incoming.

A discontinuity satisfying (3.21) and (3.22) is called a delta shock wave to the system (1.1) and (1.3), denoted by δ_S, as shown in Fig.3.2.

Under the entropy condition (3.22), via solving the generalized Rankine-Hugoniot conditions (3.21) with initial data $x^\epsilon(0) = 0$ and $w^\epsilon(0) = 0$, we have, by a trivial calculation,

$$\begin{cases} \sigma^\epsilon = u_\delta^\epsilon = \dfrac{\rho_+ u_+ - \rho_- u_- + \sqrt{\rho_-\rho_+\left((u_+ - u_-)^2 - \epsilon\left(\frac{1}{\rho_-} - \frac{1}{\rho_+}\right)\left(\frac{1}{\rho_-^\alpha} - \frac{1}{\rho_+^\alpha}\right)\right)}}{\rho_+ - \rho_-}, \\ w^\epsilon(t) = \dfrac{\sqrt{\rho_-\rho_+\left((u_+ - u_-)^2 - \epsilon\left(\frac{1}{\rho_-} - \frac{1}{\rho_+}\right)\left(\frac{1}{\rho_-^\alpha} - \frac{1}{\rho_+^\alpha}\right)\right)}}{\sqrt{1+(\sigma^\epsilon)^2}} t, \\ v_\delta^\epsilon = \dfrac{\rho_-\rho_+(u_- - u_+)(v_- - v_+)}{(\rho_+ - \rho_-)\sqrt{\rho_-\rho_+\left((u_+ - u_-)^2 - \epsilon\left(\frac{1}{\rho_-} - \frac{1}{\rho_+}\right)\left(\frac{1}{\rho_-^\alpha} - \frac{1}{\rho_+^\alpha}\right)\right)}} + \dfrac{\rho_+ v_+ - \rho_- v_-}{\rho_+ - \rho_-} \end{cases} \tag{3.23}$$

for $\rho_- \neq \rho_+$, and

$$\sigma^\epsilon = u_\delta^\epsilon = \frac{u_- + u_+}{2}, \quad w^\epsilon(t) = \frac{\rho_- u_- - \rho_+ u_+}{\sqrt{1+(\sigma^\epsilon)^2}} t, \quad v_\delta^\epsilon = \frac{v_- + v_+}{2} \tag{3.24}$$

for $\rho_- = \rho_+$.

Theorem 3.3. Under the condition $u_- - \sqrt{\epsilon}\rho_-^{-\frac{1+\alpha}{2}} \geq u_+ + \sqrt{\epsilon}\rho_+^{-\frac{1+\alpha}{2}}$, the Riemann solution to (1.1) and (1.3) admits a uniquely a delta shock wave in the form (3.20), where $w^\epsilon(t)$, u_δ^ϵ and v_δ^ϵ are shown in (3.23) for $\rho_- \neq \rho_+$ and (3.24) for $\rho_- = \rho_+$.

4. Limit of Riemann solutions to (1.1) and (1.3) for $u_- > u_+$

In this section, we investigate the concentration phenomenon in solutions. To this end, we will study the limit of Riemann solutions to the GCG equations (1.1) and (1.3). A key point is to show how the solution changes along with the values of $\epsilon \to 0$. Thus, we introduce two critical values ϵ_0 and ϵ_1, which will play important roles in the following discussion.

Lemma 4.1. For the case $u_- > u_+$, if $\rho_- = \rho_+$, then there exists an $\epsilon_0 > 0$, such that the projection of the state (ρ_+, u_+, v_+) onto the (u, ρ) plane $(\rho_+, u_+) \in V$ as $0 < \epsilon < \epsilon_0$; While if $\rho_- \neq \rho_+$, then there exist $\epsilon_1 > \epsilon_0 > 0$, such that the projection of the state (ρ_+, u_+, v_+) onto the (u, ρ) plane $(\rho_+, u_+) \in IV \cup V$ as $0 < \epsilon < \epsilon_1$, and $(\rho_+, u_+) \in V$ as $0 < \epsilon < \epsilon_0$.

Proof. Let (ρ_-, u_-) be the projection of the state (ρ_-, u_-, v_-) onto the (u, ρ) plane. Then, the state (ρ, u), which is the projection of the state (ρ, u, v) onto the (u, ρ) plane, can be connected on the right to (ρ_-, u_-) directly by a delta shock wave if and only if $u + \sqrt{\epsilon}\rho^{-\frac{1+\alpha}{2}} \leq u_- - \sqrt{\epsilon}\rho_-^{-\frac{1+\alpha}{2}}$.

If $\rho_- = \rho_+$, then $(\rho_+, u_+) \in IV \cup V$ for any $\epsilon > 0$. Moreover, $(\rho_+, u_+) \in V(\rho_-, u_-)$ if $u_+ < u_- - 2\sqrt{\epsilon}\rho_-^{-\frac{1+\alpha}{2}}$. So, we take $\epsilon_0 = \frac{(u_- - u_+)^2 \rho_-^{1+\alpha}}{4}$ and $(\rho_+, u_+) \in V$ as $0 < \epsilon < \epsilon_0$.

If $\rho_- \neq \rho_+$, we assume that $(\rho_+, u_+) \in IV$, then from the second equations in (3.13) and (3.15) for $\overleftarrow{S}$ and $\overrightarrow{S}$, it yields that $u_+ < u_- - \sqrt{\epsilon\left(\frac{1}{\rho_-} - \frac{1}{\rho_+}\right)\left(\frac{1}{\rho_-^\alpha} - \frac{1}{\rho_+^\alpha}\right)}$, from which we have

$$\epsilon < \frac{(u_- - u_+)^2}{\left(\frac{1}{\rho_-} - \frac{1}{\rho_+}\right)\left(\frac{1}{\rho_-^\alpha} - \frac{1}{\rho_+^\alpha}\right)} := \epsilon_1. \tag{4.1}$$

Obviously, $(\rho_+, u_+) \in IV \cup V$ as $0 < \epsilon < \epsilon_1$. Furthermore, let (ρ_+, u_+) be on the S_δ curve (3.16), then we can solve a critical value

$$\epsilon_0 = \left(\frac{u_- - u_+}{\rho_+^{-\frac{1+\alpha}{2}} + \rho_-^{-\frac{1+\alpha}{2}}}\right)^2. \tag{4.2}$$

Thus, when $0 < \epsilon < \epsilon_0$, one has $u_+ < u_- - \sqrt{\epsilon}\rho_-^{-\frac{1+\alpha}{2}} - \sqrt{\epsilon}\rho_+^{-\frac{1+\alpha}{2}}$, which implies that $(\rho_+, u_+) \in V$. The proof is finished. □

From the above analysis, we observe that, when $\epsilon_0 < \epsilon < \epsilon_1$, namely, $(\rho_+, u_+) \in IV$, the curves $\overleftarrow{S}$ and $\overrightarrow{S}$ will become steeper as ϵ is much smaller. At this time, since $(\rho_+, u_+) \in IV$, so the solution of (1.1) and (1.3) can be formulated as

$$(\rho_-, u_-, v_-) + \overleftarrow{S} + (\rho_*^\epsilon, u_*^\epsilon, v_{*1}^\epsilon) + J + (\rho_*^\epsilon, u_*^\epsilon, v_{*2}^\epsilon) + \overrightarrow{S} + (\rho_+, u_+, v_+), \tag{4.3}$$

which satisfies

$$\overleftarrow{S} : \begin{cases} \omega_1^\epsilon = u_- - \sqrt{\dfrac{\epsilon\rho_*^\epsilon}{\rho_-(\rho_*^\epsilon - \rho_-)} \cdot \left(\dfrac{1}{\rho_-^\alpha} - \dfrac{1}{(\rho_*^\epsilon)^\alpha}\right)}, \\ u_*^\epsilon = u_- - \sqrt{\epsilon\left(\dfrac{1}{\rho_-} - \dfrac{1}{\rho_*^\epsilon}\right)\left(\dfrac{1}{\rho_-^\alpha} - \dfrac{1}{(\rho_*^\epsilon)^\alpha}\right)}, \quad \rho_*^\epsilon > \rho_-, \\ v_{*1}^\epsilon = v_-. \end{cases} \tag{4.4}$$

$$J:\ \omega_2^\epsilon = u_*^\epsilon, \quad v_{*1}^\epsilon \neq v_{*2}^\epsilon, \tag{4.5}$$

$$\overrightarrow{S}: \begin{cases} \omega_3^\epsilon = u_*^\epsilon + \sqrt{\dfrac{\epsilon\rho_+}{\rho_*^\epsilon(\rho_+ - \rho_*^\epsilon)} \cdot \left(\dfrac{1}{(\rho_*^\epsilon)^\alpha} - \dfrac{1}{\rho_+^\alpha}\right)}, \\ u_+ = u_*^\epsilon - \sqrt{\epsilon\left(\dfrac{1}{\rho_*^\epsilon} - \dfrac{1}{\rho_+}\right)\left(\dfrac{1}{(\rho_*^\epsilon)^\alpha} - \dfrac{1}{\rho_+^\alpha}\right)}, \quad \rho_*^\epsilon > \rho_+, \\ v_{*2}^\epsilon = v_+. \end{cases} \tag{4.6}$$

Here, ω_1^ϵ, ω_2^ϵ and ω_3^ϵ are the propagation velocity of $\overleftarrow{S}$, J and $\overrightarrow{S}$, respectively.

We now give some lemmas to show the limit behavior of solutions to (1.1) as $\epsilon \to \epsilon_0$.

Lemma 4.2. $\lim_{\epsilon\to\epsilon_0} \rho_*^\epsilon = +\infty$.

Proof. Together with the second equations of (4.4) and (4.6), we have

$$u_- - u_+ = \sqrt{\epsilon\left(\frac{1}{\rho_-} - \frac{1}{\rho_*^\epsilon}\right)\left(\frac{1}{\rho_-^\alpha} - \frac{1}{(\rho_*^\epsilon)^\alpha}\right)} + \sqrt{\epsilon\left(\frac{1}{\rho_*^\epsilon} - \frac{1}{\rho_+}\right)\left(\frac{1}{(\rho_*^\epsilon)^\alpha} - \frac{1}{\rho_+^\alpha}\right)}, \quad \rho_*^\epsilon > \rho_\pm,$$

from which, by taking $\epsilon \to \epsilon_0$ on both sides, one has

$$u_- - u_+ = \lim_{\epsilon\to\epsilon_0}\left(\sqrt{\epsilon\left(\frac{1}{\rho_-} - \frac{1}{\rho_*^\epsilon}\right)\left(\frac{1}{\rho_-^\alpha} - \frac{1}{(\rho_*^\epsilon)^\alpha}\right)} + \sqrt{\epsilon\left(\frac{1}{\rho_*^\epsilon} - \frac{1}{\rho_+}\right)\left(\frac{1}{(\rho_*^\epsilon)^\alpha} - \frac{1}{\rho_+^\alpha}\right)}\right).$$

Thus, from $\epsilon_0 = \left(\frac{u_- - u_+}{\rho_+^{-\frac{1+\alpha}{2}} + \rho_-^{-\frac{1+\alpha}{2}}}\right)^2$, one has $\lim_{\epsilon\to\epsilon_0} \rho_*^\epsilon = +\infty$. The proof is completed. □

Lemma 4.3. It holds that

$$\lim_{\epsilon\to\epsilon_0} u_*^\epsilon = \lim_{\epsilon\to\epsilon_0} \omega_1^\epsilon = \lim_{\epsilon\to\epsilon_0} \omega_2^\epsilon = \lim_{\epsilon\to\epsilon_0} \omega_3^\epsilon = \frac{u_-\rho_-^{-\frac{1+\alpha}{2}} + u_+\rho_+^{-\frac{1+\alpha}{2}}}{\rho_-^{-\frac{1+\alpha}{2}} + \rho_+^{-\frac{1+\alpha}{2}}} := \sigma. \tag{4.7}$$

Proof. By virtue of the first two equations of (4.4) and Lemma 4.2, we have

$$\lim_{\epsilon\to\epsilon_0} u_*^\epsilon = u_- - \lim_{\epsilon\to\epsilon_0}\sqrt{\epsilon\left(\frac{1}{\rho_-} - \frac{1}{\rho_*^\epsilon}\right)\left(\frac{1}{\rho_-^\alpha} - \frac{1}{(\rho_*^\epsilon)^\alpha}\right)} = u_- - \frac{(u_- - u_+)\cdot\rho_-^{-\frac{1+\alpha}{2}}}{\rho_+^{-\frac{1+\alpha}{2}} + \rho_-^{-\frac{1+\alpha}{2}}} = \sigma,$$

and

$$\lim_{\epsilon\to\epsilon_0} \omega_1^\epsilon = u_- - \lim_{\epsilon\to\epsilon_0}\sqrt{\epsilon\cdot\frac{1}{\rho_-^{\alpha+1}}} = u_- - \frac{(u_- - u_+)\cdot\rho_-^{-\frac{1+\alpha}{2}}}{\rho_+^{-\frac{1+\alpha}{2}} + \rho_-^{-\frac{1+\alpha}{2}}} = \sigma.$$

Similarly, from (4.5) and (4.6) one can prove $\lim_{\epsilon\to\epsilon_0} \omega_2^\epsilon = \lim_{\epsilon\to\epsilon_0} \omega_3^\epsilon = \sigma$. Thus, Lemma 4.3 is right. □

Lemma 4.4.

$$\lim_{\epsilon\to\epsilon_0} \rho_*^\epsilon(\omega_2^\epsilon - \omega_1^\epsilon) = \rho_-(u_- - \sigma), \quad \lim_{\epsilon\to\epsilon_0} \rho_*^\epsilon(\omega_3^\epsilon - \omega_2^\epsilon) = \rho_+(\sigma - u_+),$$

and

$$\lim_{\epsilon\to\epsilon_0}\rho_*^\epsilon(\omega_3^\epsilon-\omega_1^\epsilon)=\sigma[\rho]-[\rho u],\quad \lim_{\epsilon\to\epsilon_0}\rho_*^\epsilon u_*^\epsilon(\omega_3^\epsilon-\omega_1^\epsilon)=\sigma[\rho u]-\left[\rho u^2-\frac{\epsilon_0}{\rho^\alpha}\right].$$

Proof. From the velocity relation for $\overleftarrow{S}$ and J, one has

$$\omega_1^\epsilon(\rho_*^\epsilon-\rho_-)=\rho_*^\epsilon u_*^\epsilon-\rho_-u_-,\quad \omega_2^\epsilon=u_*^\epsilon,$$

from which one has $\lim_{\epsilon\to\epsilon_0}\rho_*^\epsilon(\omega_2^\epsilon-\omega_1^\epsilon)=\lim_{\epsilon\to\epsilon_0}(\rho_-u_--\rho_-\omega_1^\epsilon)=\rho_-(u_--\sigma)$. Similarly, we obtain from the velocity relation for J and $\overrightarrow{S}$ that $\lim_{\epsilon\to\epsilon_0}\rho_*^\epsilon(\omega_3^\epsilon-\omega_2^\epsilon)=\rho_+(\sigma-u_+)$. As a result, we have

$$\lim_{\epsilon\to\epsilon_0}\rho_*^\epsilon(\omega_3^\epsilon-\omega_1^\epsilon)=\lim_{\epsilon\to\epsilon_0}\rho_*^\epsilon(\omega_3^\epsilon-\omega_2^\epsilon)+\lim_{\epsilon\to\epsilon_0}\rho_*^\epsilon(\omega_2^\epsilon-\omega_1^\epsilon)=\sigma[\rho]-[\rho u].$$

Moreover, it yields from the Rankine-Hugoniot relation (3.9) for $\overleftarrow{S}$ and $\overrightarrow{S}$ that

$$\begin{cases}\omega_1^\epsilon(\rho_*^\epsilon u_*^\epsilon-\rho_-u_-)=\rho_*^\epsilon(u_*^\epsilon)^2-\rho_-u_-^2-\dfrac{\epsilon}{(\rho_*^\epsilon)^\alpha}+\dfrac{\epsilon}{\rho_-^\alpha},\\ \omega_3^\epsilon(\rho_+u_+-\rho_*^\epsilon u_*^\epsilon)=\rho_+u_+^2-\rho_*^\epsilon(u_*^\epsilon)^2-\dfrac{\epsilon}{\rho_+^\alpha}+\dfrac{\epsilon}{(\rho_*^\epsilon)^\alpha},\end{cases}$$

which leads to

$$\lim_{\epsilon\to\epsilon_0}\rho_*^\epsilon u_*^\epsilon(\omega_3^\epsilon-\omega_1^\epsilon)=\sigma[\rho u]-\left[\rho u^2-\frac{\epsilon_0}{\rho^\alpha}\right].$$

This is the end of the proof. □

Lemmas 4.2-4.4 imply that, as $\epsilon\to\epsilon_0$, the two shocks $\overleftarrow{S}$ and $\overrightarrow{S}$ and the contact discontinuity J coincide, and the intermediate density ρ_*^ϵ becomes singular. Let us give the following result which gives a very nice depiction of the limit in the case $u_->u_+$.

Theorem 4.1. Let $u_->u_+$. For each fixed $\epsilon\in(\epsilon_0,\epsilon_1)$, assume that $(\rho^\epsilon,u^\epsilon,v^\epsilon)$ is a solution of (1.1) and (1.3) with (1.5), which consists of two shocks $\overleftarrow{S}$, $\overrightarrow{S}$ and a contact discontinuity J as constructed in Section 3. Then, ρ^ϵ, $\rho^\epsilon u^\epsilon$ and $\rho^\epsilon v^\epsilon$ converge in the sense of distributions as $\epsilon\to\epsilon_0$, and the limit functions ρ, ρu and ρv are the sums of a step function and a Dirac delta function with weights

$$\frac{t}{\sqrt{1+\sigma^2}}\left(\sigma[\rho]-[\rho u]\right),\quad \frac{t}{\sqrt{1+\sigma^2}}\left(\sigma[\rho u]-\left[\rho u^2-\frac{\epsilon_0}{\rho^\alpha}\right]\right),\quad \frac{t}{\sqrt{1+\sigma^2}}\left(\sigma[\rho v]-[\rho uv]\right),$$

respectively, in which $\sigma=\frac{u_-\rho_-^{-\frac{1+\alpha}{2}}+u_+\rho_+^{-\frac{1+\alpha}{2}}}{\rho_-^{-\frac{1+\alpha}{2}}+\rho_+^{-\frac{1+\alpha}{2}}}$.

Proof. (i). Set $\xi=x/t$. For each fixed $\epsilon\in(\epsilon_0,\epsilon_1)$, the solution of (1.1) reads

$$(\rho^\epsilon,u^\epsilon,v^\epsilon)(\xi)=\begin{cases}(\rho_-,u_-,v_-), & \xi<\omega_1^\epsilon,\\ (\rho_*^\epsilon,u_*^\epsilon,v_{*1}^\epsilon), & \omega_1^\epsilon<\xi<\omega_2^\epsilon,\\ (\rho_*^\epsilon,u_*^\epsilon,v_{*2}^\epsilon), & \omega_2^\epsilon<\xi<\omega_3^\epsilon,\\ (\rho_+,u_+,v_+), & \xi>\omega_3^\epsilon,\end{cases}\tag{4.8}$$

in which ρ_*^ϵ, u_*^ϵ, v_{*1}^ϵ, v_{*2}^ϵ are constants only depend on ϵ, and $v_{*1}^\epsilon=v_-$, $v_{*2}^\epsilon=v_+$.

Moreover, for any test function $\phi \in C_0^\infty(-\infty, +\infty)$, the solution (4.8) satisfies

$$-\int_{-\infty}^{+\infty} \rho^\epsilon (u^\epsilon - \xi)\phi' d\xi + \int_{-\infty}^{+\infty} \rho^\epsilon \phi d\xi = 0, \tag{4.9}$$

$$-\int_{-\infty}^{+\infty} \rho^\epsilon u^\epsilon (u^\epsilon - \xi)\phi' d\xi + \int_{-\infty}^{+\infty} \frac{\epsilon}{(\rho^\epsilon)^\alpha}\phi' d\xi + \int_{-\infty}^{+\infty} \rho^\epsilon u^\epsilon \phi d\xi = 0 \tag{4.10}$$

and

$$-\int_{-\infty}^{+\infty} \rho^\epsilon v^\epsilon (u^\epsilon - \xi)\phi' d\xi + \int_{-\infty}^{+\infty} \rho^\epsilon v^\epsilon \phi d\xi = 0. \tag{4.11}$$

(ii). Let us discuss the limits of $\rho^\epsilon u^\epsilon$, $\rho^\epsilon v^\epsilon$ and ρ^ϵ depending on ξ. For the first integral on the left of (4.10), we have

$$\int_{-\infty}^{+\infty} \rho^\epsilon u^\epsilon (u^\epsilon - \xi)\phi' d\xi = \left(\int_{-\infty}^{\omega_1^\epsilon} + \int_{\omega_1^\epsilon}^{\omega_2^\epsilon} + \int_{\omega_2^\epsilon}^{\omega_3^\epsilon} + \int_{\omega_3^\epsilon}^{+\infty} \right) \rho^\epsilon u^\epsilon (u^\epsilon - \xi)\phi' d\xi. \tag{4.12}$$

For the first and last terms on the right of (4.12), it can be calculated that

$$\lim_{\epsilon \to \epsilon_0} \left(\int_{-\infty}^{\omega_1^\epsilon} + \int_{\omega_3^\epsilon}^{+\infty} \right) \rho^\epsilon u^\epsilon (u^\epsilon - \xi)\phi' d\xi = (\sigma[\rho u] - [\rho u^2])\phi(\sigma) + \int_{-\infty}^{+\infty} H_2(\xi - \sigma)\phi d\xi, \tag{4.13}$$

where $H_2(\xi - \sigma) = \rho_\pm u_\pm$, $\pm(\xi - \sigma) > 0$.

While for the second and third terms on the right of (4.12), the limit of which when $\epsilon \to \epsilon_0$ equals

$$\begin{aligned}
&\lim_{\epsilon \to \epsilon_0} \int_{\omega_1^\epsilon}^{\omega_2^\epsilon} \rho_*^\epsilon u_*^\epsilon (u_*^\epsilon - \xi)\phi' d\xi + \lim_{\epsilon \to \epsilon_0} \int_{\omega_2^\epsilon}^{\omega_3^\epsilon} \rho_*^\epsilon u_*^\epsilon (u_*^\epsilon - \xi)\phi' d\xi = \lim_{\epsilon \to \epsilon_0} \int_{\omega_1^\epsilon}^{\omega_3^\epsilon} \rho_*^\epsilon u_*^\epsilon (u_*^\epsilon - \xi)\phi' d\xi \\
&= \lim_{\epsilon \to \epsilon_0} \rho_*^\epsilon u_*^\epsilon (\omega_3^\epsilon - \omega_1^\epsilon) \cdot \left(\frac{\phi(\omega_3^\epsilon) - \phi(\omega_1^\epsilon)}{\omega_3^\epsilon - \omega_1^\epsilon} u_*^\epsilon - \frac{\omega_3^\epsilon \phi(\omega_3^\epsilon) - \omega_1^\epsilon \phi(\omega_1^\epsilon)}{\omega_3^\epsilon - \omega_1^\epsilon} + \frac{1}{\omega_3^\epsilon - \omega_1^\epsilon} \int_{\omega_1^\epsilon}^{\omega_3^\epsilon} \phi d\xi \right) \\
&= \left(\sigma[\rho u] - \left[\rho u^2 - \frac{\epsilon_0}{\rho^\alpha} \right] \right) \Big(\sigma\phi'(\sigma) - \sigma\phi'(\sigma) - \phi(\sigma) + \phi(\sigma) \Big) \\
&= 0.
\end{aligned} \tag{4.14}$$

From (4.13) and (4.14), it follows that

$$\lim_{\epsilon \to \epsilon_0} \int_{-\infty}^{+\infty} \rho^\epsilon u^\epsilon (u^\epsilon - \xi)\phi' d\xi = (\sigma[\rho u] - [\rho u^2])\phi(\sigma) + \int_{-\infty}^{+\infty} H_2(\xi - \sigma)\phi d\xi. \tag{4.15}$$

We turn to the second term on the left of (4.10), one has

$$\lim_{\epsilon\to\epsilon_0}\int_{-\infty}^{+\infty}\frac{\epsilon}{(\rho^\epsilon)^\alpha}=\lim_{\epsilon\to\epsilon_0}\left(\int_{-\infty}^{\omega_1^\epsilon}\frac{\epsilon}{\rho_-^\alpha}\phi' d\xi+\int_{\omega_1^\epsilon}^{\omega_2^\epsilon}\frac{\epsilon}{(\rho_*^\epsilon)^\alpha})\phi' d\xi+\int_{\omega_2^\epsilon}^{\omega_3^\epsilon}\frac{\epsilon}{(\rho_*^\epsilon)^\alpha}\phi' d\xi+\int_{\omega_3^\epsilon}^{+\infty}\frac{\epsilon}{\rho_+^\alpha}\phi' d\xi\right)$$

$$=\lim_{\epsilon\to\epsilon_0}\left(\frac{\epsilon}{\rho_-^\alpha}\phi(\omega_1)-\frac{\epsilon}{\rho_+^\alpha}\phi(\omega_3)+\frac{\epsilon}{(\rho_*^\epsilon)^\alpha}\Big(\phi(\omega_3)-\phi(\omega_1)\Big)\right)$$

$$=-\left[\frac{\epsilon_0}{\rho^\alpha}\right]\phi(\sigma). \tag{4.16}$$

Thereby, by substituting (4.15) and (4.16) into (4.10), we immediately obtain that

$$\lim_{\epsilon\to\epsilon_0}\int_{-\infty}^{+\infty}\Big(\rho^\epsilon u^\epsilon-H_2(\xi-\sigma)\Big)\phi d\xi=\left(\sigma[\rho u]-\left[\rho u^2-\frac{\epsilon_0}{\rho^\alpha}\right]\right)\phi(\sigma), \tag{4.17}$$

for any test function $\phi\in C_0^\infty(-\infty,+\infty)$.

Let us turn to (4.11). For the first term on the left of (4.11), it can be written as

$$\lim_{\epsilon\to\epsilon_0}\int_{-\infty}^{+\infty}\rho^\epsilon v^\epsilon(u^\epsilon-\xi)\phi' d\xi=\lim_{\epsilon\to\epsilon_0}\left(\int_{-\infty}^{\omega_1^\epsilon}+\int_{\omega_1^\epsilon}^{\omega_2^\epsilon}+\int_{\omega_2^\epsilon}^{\omega_3^\epsilon}+\int_{\omega_3^\epsilon}^{+\infty}\right)\rho^\epsilon v^\epsilon(u^\epsilon-\xi)\phi' d\xi \tag{4.18}$$

The first and last terms on the right of (4.18) can be calculated as

$$\lim_{\epsilon\to\epsilon_0}\left(\int_{-\infty}^{\omega_1^\epsilon}+\int_{\omega_3^\epsilon}^{+\infty}\right)\rho^\epsilon v^\epsilon(u^\epsilon-\xi)\phi' d\xi=(\sigma[\rho v]-[\rho uv])\phi(\sigma)+\int_{-\infty}^{+\infty}H_3(\xi-\sigma)\phi d\xi, \tag{4.19}$$

where $H_3(\xi-\sigma)=\rho_\pm v_\pm$, $\pm(\xi-\sigma)>0$.

While for the middle two terms on the right of (4.18), noting that

$$\int_{\omega_1^\epsilon}^{\omega_2^\epsilon}\rho_*^\epsilon v_-(u_*^\epsilon-\xi)\phi' d\xi+\int_{\omega_2^\epsilon}^{\omega_3^\epsilon}\rho_*^\epsilon v_+(u_*^\epsilon-\xi)\phi' d\xi$$

$$=-\rho_*^\epsilon v_-(\omega_2^\epsilon-\omega_1^\epsilon)\left(\phi(\omega_1^\epsilon)-\frac{1}{\omega_2^\epsilon-\omega_1^\epsilon}\int_{\omega_1^\epsilon}^{\omega_2^\epsilon}\phi d\xi\right)-\rho_*^\epsilon v_+(\omega_3^\epsilon-\omega_2^\epsilon)\left(\phi(\omega_3^\epsilon)-\frac{1}{\omega_3^\epsilon-\omega_2^\epsilon}\int_{\omega_2^\epsilon}^{\omega_3^\epsilon}\phi d\xi\right),$$

which converges to $-\rho_-v_-(u_--\sigma)\big(\phi(\sigma)-\phi(\sigma)\big)-\rho_+v_+(\sigma-u_+)\big(\phi(\sigma)-\phi(\sigma)\big)=0$ according to Lemma 4.4. So, using (4.18) and (4.19) again, we have

$$\lim_{\epsilon\to\epsilon_0}\int_{-\infty}^{+\infty}\rho^\epsilon v^\epsilon(u^\epsilon-\xi)\phi' d\xi=(\sigma[\rho v]-[\rho uv])\phi(\sigma)+\int_{-\infty}^{+\infty}H_3(\xi-\sigma)\phi d\xi. \tag{4.20}$$

Taking (4.20) into (4.11) yields that

$$\int_{-\infty}^{+\infty}\big(\rho^\epsilon v^\epsilon-H_3(\xi-\sigma)\big)\phi d\xi=(\sigma[\rho v]-[\rho uv])\phi(\sigma). \tag{4.21}$$

In a similar manner, from (4.9), we can prove that

$$\lim_{\epsilon\to\epsilon_0}\int\limits_{-\infty}^{+\infty}\Big(\rho^\epsilon-H_1(\xi-\sigma)\Big)\phi d\xi=\Big(\sigma[\rho]-[\rho u]\Big)\phi(\sigma), \tag{4.22}$$

where $H_1(\xi-\sigma)=\rho_\pm$, $\pm(\xi-\sigma)>0$.

(iii). Finally, we check the limits of ρ^ϵ, $\rho^\epsilon u^\epsilon$ and $\rho^\epsilon v^\epsilon$ by tracing the time-dependence of weights of the δ-measure as $\epsilon\to\epsilon_0$. Then, for any $\psi(t,x)\in C_0^\infty(R^+\times R^1)$, we have

$$\begin{aligned}&\lim_{\epsilon\to\epsilon_0}\int\limits_0^{+\infty}\int\limits_{-\infty}^{+\infty}\rho^\epsilon(x/t)u^\epsilon(x/t)\psi(t,x)dxdt\\&=\int\limits_0^{+\infty}t\left(\left(\sigma[\rho u]-\left[\rho u^2-\frac{\epsilon_0}{\rho^\alpha}\right]\right)\psi(t,\sigma t)+\int\limits_{-\infty}^{+\infty}H_2(\xi-\sigma)\psi(t,\xi t)d\xi\right)dt\\&=\int\limits_0^{+\infty}\int\limits_{-\infty}^{+\infty}H_2(x-\sigma t)\psi(t,x)dxdt+\big\langle w_2(\cdot)\delta_S,\psi(\cdot,\cdot)\big\rangle\end{aligned} \tag{4.23}$$

by using (4.17), in which

$$w_2(t)=\frac{t}{\sqrt{1+\sigma^2}}\left(\sigma[\rho u]-\left[\rho u^2-\frac{\epsilon_0}{\rho^\alpha}\right]\right),$$

according to the Definition 2.1.

Analogously, we can conclude that

$$\lim_{\epsilon\to\epsilon_0}\int\limits_0^{+\infty}\int\limits_{-\infty}^{+\infty}\rho^\epsilon(x/t)\psi(t,x)dxdt=\int\limits_0^{+\infty}\int\limits_{-\infty}^{+\infty}H_1(x-\sigma t)\psi(t,x)dxdt+\big\langle w_1(\cdot)\delta_S,\psi(\cdot,\cdot)\big\rangle, \tag{4.24}$$

in which $w_1(t)=\frac{t}{\sqrt{1+\sigma^2}}(\sigma[\rho]-[\rho u])$, and

$$\lim_{\epsilon\to\epsilon_0}\int\limits_0^{+\infty}\int\limits_{-\infty}^{+\infty}\rho^\epsilon v^\epsilon(x/t)\psi(t,x)dxdt=\int\limits_0^{+\infty}\int\limits_{-\infty}^{+\infty}H_3(x-\sigma t)\psi(t,x)dxdt+\big\langle w_3(\cdot)\delta_S,\psi(\cdot,\cdot)\big\rangle \tag{4.25}$$

with $w_3(t)=\frac{t}{\sqrt{1+\sigma^2}}(\sigma[\rho v]-[\rho uv])$. We finish the proof of Theorem 4.1. □

Theorem 4.2. If $u_->u_+$ and the projection of the state (ρ_+,u_+,v_+) onto the (ρ,u) phase plane $(\rho_+,u_+)\in V$, then the limit of the delta shock wave of (1.1) and (1.3) with (1.5) when $\epsilon\to0$ is a delta shock wave solution of the PGD model (1.4) with the same initial data.

Proof. When $(\rho_+,u_+)\in V$, the delta shock wave solution of (1.1) and (1.3) with (1.5) is expressed in (3.23) and (3.24). Then, it is easily checked that

$$\begin{aligned}\lim_{\epsilon\to0}\sigma^\epsilon=\lim_{\epsilon\to0}u_\delta^\epsilon&=\lim_{\epsilon\to0}\frac{\rho_+u_+-\rho_-u_-+\sqrt{\rho_-\rho_+\left((u_+-u_-)^2-\epsilon\left(\frac{1}{\rho_-}-\frac{1}{\rho_+}\right)\left(\frac{1}{\rho_-^\alpha}-\frac{1}{\rho_+^\alpha}\right)\right)}}{\rho_+-\rho_-}\\&=\frac{\sqrt{\rho_-}u_-+\sqrt{\rho_+}u_+}{\sqrt{\rho_-}+\sqrt{\rho_+}}=\sigma_0,\end{aligned}$$

$$\lim_{\epsilon\to0} w^\epsilon = \lim_{\epsilon\to0}\frac{\sqrt{\rho_-\rho_+\left((u_+-u_-)^2-\epsilon\left(\frac{1}{\rho_-}-\frac{1}{\rho_+}\right)\left(\frac{1}{\rho_-^\alpha}-\frac{1}{\rho_+^\alpha}\right)\right)}}{\sqrt{1+(\sigma^\epsilon)^2}}t = \frac{\sqrt{\rho_-\rho_+}(u_--u_+)}{\sqrt{1+\sigma_0^2}}t,$$

$$\lim_{\epsilon\to0} v_\delta^\epsilon = \lim_{\epsilon\to0}\left(\frac{\rho_-\rho_+(u_--u_+)(v_--v_+)}{(\rho_+-\rho_-)\sqrt{\rho_-\rho_+\left((u_+-u_-)^2-\epsilon\left(\frac{1}{\rho_-}-\frac{1}{\rho_+}\right)\left(\frac{1}{\rho_-^\alpha}-\frac{1}{\rho_+^\alpha}\right)\right)}}+\frac{\rho_+v_+-\rho_-v_-}{\rho_+-\rho_-}\right)$$

$$= \frac{\sqrt{\rho_-}v_-+\sqrt{\rho_+}v_+}{\sqrt{\rho_-}+\sqrt{\rho_+}},$$

for $\rho_-\neq\rho_+$, and

$$\lim_{\epsilon\to0}\sigma^\epsilon = \lim_{\epsilon\to0}\frac{u_-+u_+}{2},\ \lim_{\epsilon\to0} w^\epsilon(t) = \lim_{\epsilon\to0}\frac{\rho_-u_--\rho_+u_+}{\sqrt{1+(\sigma^\epsilon)^2}}t = \frac{\rho_-u_--\rho_+u_+}{\sqrt{1+\sigma_0^2}}t,\ \lim_{\epsilon\to0} v_\delta^\epsilon = \frac{v_-+v_+}{2}$$

for $\rho_-=\rho_+$. Clearly, the limits of delta-shock solutions to (1.1) and (1.3) are in accordance with the delta-shock solutions (2.11) and (2.12), as proposed for the PGD model (1.4). The proof for Theorem 4.2 is finished. □

Remark 4.1. Similar to [25, 30, 33], when $(\rho_+,u_+)\in IV$, the limit of Riemann solutions to the GCG equations (1.1) and (1.3) as $\epsilon\to\epsilon_0$ is nothing but the delta-shock solution of (1.1) and (1.3) itself in the case $(\rho_+,u_+)\in S_\delta$, where the curve S_δ is actually the boundary between the regions IV and V. From the results of this section, we conclude that the two shocks $\overleftarrow{S}$, $\overrightarrow{S}$ and possibly a contact discontinuity J coincide as a delta shock wave of (1.1) and (1.3) itself when ϵ decreases to a certain critical value ϵ_0. Moreover, as ϵ continues to drop and in the end, tends to zero, the delta shock solution is just that of the PGD model (1.4). Form this point of view, our results can be regarded as a generalization of [25, 33].

5. Limit of Riemann solutions to (1.1) and (1.3) for $u_-<u_+$

In this section, we analyze the cavitation phenomenon. To this end, we need to discuss the limit behavior of solutions to the Riemann problem (1.1), (1.3) and (1.5) for $u_-<u_+$.

Lemma 5.1. If $u_-<u_+$, then there exists some $\tilde{\epsilon}_0$ such that the projection of the state (ρ_+,u_+,v_+) onto the (ρ,u) phase plane satisfies $(\rho_+,u_+)\in I$ when $0<\epsilon<\tilde{\epsilon}_0$.

Proof. The conclusion is true for arbitrary $\epsilon>0$ if $\rho_-=\rho_+$. While if $\rho_-\neq\rho_+$, we assume that $(\rho_+,u_+)\in I$, then one has

$$u_+>u_-+\frac{2\sqrt{\epsilon\alpha}}{1+\alpha}\left(\rho_+^{-\frac{1+\alpha}{2}}-\rho_-^{-\frac{1+\alpha}{2}}\right)$$

and

$$u_+>u_--\frac{2\sqrt{\epsilon\alpha}}{1+\alpha}\left(\rho_+^{-\frac{1+\alpha}{2}}-\rho_-^{-\frac{1+\alpha}{2}}\right),$$

which yields that

$$\epsilon<\left(\frac{(1+\alpha)(u_--u_+)}{2\sqrt{\alpha}\left(\rho_+^{-\frac{1+\alpha}{2}}-\rho_-^{-\frac{1+\alpha}{2}}\right)}\right)^2 := \tilde{\epsilon}_0. \tag{5.1}$$

Obviously, $(\rho_+, u_+) \in I$ as $0 < \epsilon < \tilde{\epsilon}_0$. Then the desired conclusion is reached. $\square$

Now, for $0 < \epsilon < \tilde{\epsilon}_0$, the solution of (1.1) and (1.3) with (1.5) can be formulated as

$$(\rho_-, u_-, v_-) + \overleftarrow{R} + (\rho_*^\epsilon, u_*^\epsilon, v_{*1}^\epsilon) + J + (\rho_*^\epsilon, u_*^\epsilon, v_{*2}^\epsilon) + \overrightarrow{R} + (\rho_+, u_+, v_+), \tag{5.2}$$

which satisfies

$$\overleftarrow{R}: \begin{cases} \xi = \lambda_1^\epsilon = u - \sqrt{\epsilon\alpha}\rho^{-\frac{1+\alpha}{2}}, \\ u_*^\epsilon - \dfrac{2\sqrt{\epsilon\alpha}}{1+\alpha}(\rho_*^\epsilon)^{-\frac{1+\alpha}{2}} = u_- - \dfrac{2\sqrt{\epsilon\alpha}}{1+\alpha}\rho_-^{-\frac{1+\alpha}{2}}, \quad \rho_*^\epsilon < \rho_-, \\ v_{*1}^\epsilon = v_-, \end{cases} \tag{5.3}$$

$$J: \xi = \lambda_2^\epsilon = u_*^\epsilon, \quad v_{*1}^\epsilon = v_-, \quad v_{*2}^\epsilon = v_+, \tag{5.4}$$

and

$$\overrightarrow{R}: \begin{cases} \xi = \lambda_3^\epsilon = u + \sqrt{\epsilon\alpha}\rho^{-\frac{1+\alpha}{2}}, \\ u_+ + \dfrac{2\sqrt{\epsilon\alpha}}{1+\alpha}\rho_+^{-\frac{1+\alpha}{2}} = u_*^\epsilon + \dfrac{2\sqrt{\epsilon\alpha}}{1+\alpha}(\rho_*^\epsilon)^{-\frac{1+\alpha}{2}}, \quad \rho_*^\epsilon < \rho_+, \\ v_{*2}^\epsilon = v_+. \end{cases} \tag{5.5}$$

Here, λ_1^ϵ, λ_2^ϵ and λ_3^ϵ are the propagation velocity of $\overleftarrow{R}$, J and $\overrightarrow{R}$, respectively.

Eliminating u_*^ϵ from the second equations of (5.3) and (5.5) gives

$$\rho_*^\epsilon = \left(\frac{(1+\alpha)(u_+ - u_-)}{4\sqrt{\epsilon\alpha}} + \frac{1}{2}\left(\rho_+^{-\frac{1+\alpha}{2}} + \rho_-^{-\frac{1+\alpha}{2}}\right)\right)^{-\frac{2}{1+\alpha}}, \tag{5.6}$$

from which we immediately deduce

$$\lim_{\epsilon \to 0} \rho_*^\epsilon = 0, \tag{5.7}$$

that is, the vacuum occurs.

In addition, it directly yields from the first equations of (5.3) and (5.5) that

$$\lim_{\epsilon \to 0} \lambda_1^\epsilon(\rho_-, u_-, v_-) = \lim_{\epsilon \to 0} \lambda_1^\epsilon(\rho_*^\epsilon, u_*^\epsilon, v_{*1}^\epsilon) = u_- \tag{5.8}$$

and

$$\lim_{\epsilon \to 0} \lambda_3^\epsilon(\rho_*^\epsilon, u_*^\epsilon, v_{*2}^\epsilon) = \lim_{\epsilon \to 0} \lambda_3^\epsilon(\rho_+, u_+, v_+) = u_+. \tag{5.9}$$

That is to say, as $\epsilon \to 0$, the two rarefaction waves $\overleftarrow{R}$, $\overrightarrow{R}$ and possibly a contact discontinuity J become the contact discontinuities of the PGD model (1.4).

We conclude the following theorem.

Theorem 5.1. Let $u_- < u_+$. For each fixed $\epsilon \in (0, \tilde{\epsilon}_0)$, assume that $(\rho^\epsilon, u^\epsilon, v^\epsilon)$ is a solution of (1.1) and (1.3) consisting of two rarefaction waves $\overleftarrow{R}$, $\overrightarrow{R}$ and a contact discontinuity J, as constructed in Section 3. Then, as $\epsilon \to 0$, the two rarefaction waves and possibly one contact discontinuity become two contact discontinuities connecting the constant states $(\rho_\pm, u_\pm, v_\pm)$ and vacuum state ($\rho = 0$), which form a vacuum solution of the PGD model (1.4).

6. Numerical simulations

We in this section present some representative numerical simulations to show the validity of concentration and cavitation studied in Sections 4-5. Many more numerical tests have been performed to make sure that what are presented are not numerical artifacts. To discretize the system, we employ the second-order non-oscillatory central schemes [15] with 150×150 cells and CFL=0.475. For convenience, we take $\alpha = 0.5$ in (1.1) and (1.3).

Case 1. $u_- > u_+$. For this case, the initial data are selected as

$$\text{Data 1:}\;\; (\rho, u, v)(0, x) = \begin{cases} (0.15, 0.20, -0.10), & x < 0, \\ (0.50, -0.35, 0.08), & x > 0. \end{cases}$$

Then, we get from (4.2) that $\epsilon_0 \approx 0.0089$ for this group of initial data. The numerical results with $\epsilon = 1$, $\epsilon = 0.0089$ and $\epsilon = 0.001$ at $t = 0.3$ are presented in Figs.6.1-6.3 to show the influence of the perturbed parameter ϵ on the formation of delta shock wave.

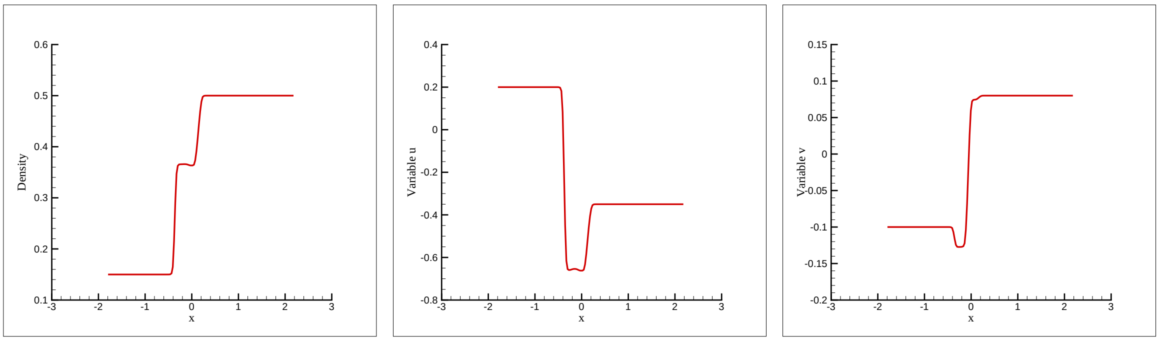

Fig.6.1. Numerical results of ρ, u and v for Data 1 at $\epsilon = 1$.

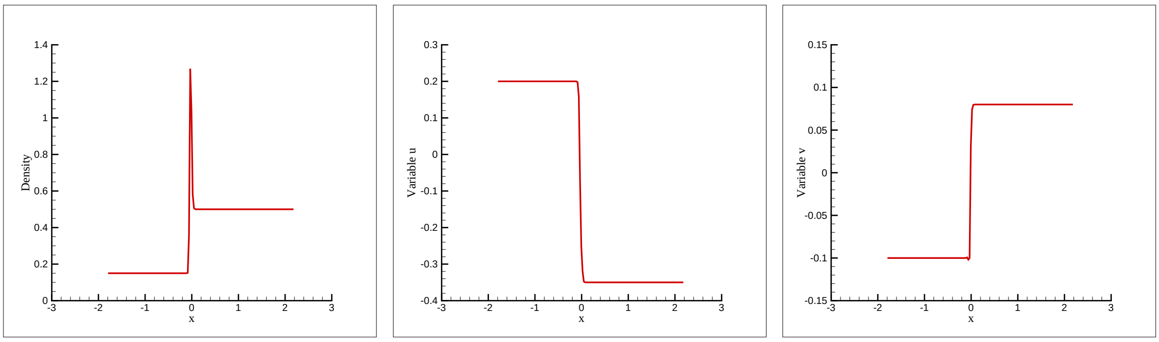

Fig.6.2. Numerical results of ρ, u and v for Data 1 at $\epsilon = 0.0089$.

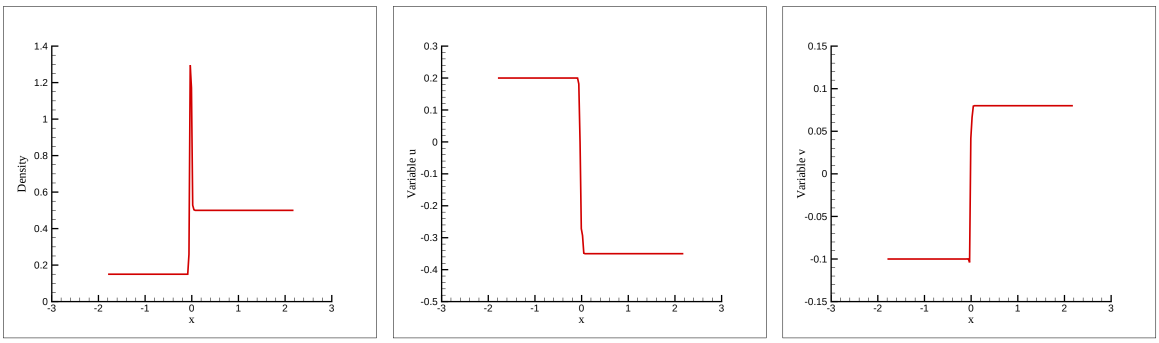

Fig.6.3. Numerical results of ρ, u and v for Data 1 at $\epsilon = 0.001$.

It is clearly observed that, there is no concentration in the solution of (1.1) as $\epsilon = 1$, that is, for a fluid with strong pressure, no concentration occurs generally. However, as ϵ drops to ϵ_0 approximately, the velocities u and v become step functions and the intermediate density ρ_*^ϵ increases dramatically, namely, the concentration occurs. Finally, as $\epsilon \to 0$, the concentration of density ρ_*^ϵ leads to a delta shock wave in the limit, and the changes of velocities u and v yield two step functions. Therefore, the delta shock wave of the PGD model (1.4) is really the limit of the delta shock wave of the GCG equations (1.1) as $\epsilon \to 0$.

Case 2. $u_- < u_+$. In this situation, the initial data are chosen as

$$\text{Data 2:}\quad (\rho, u, v)(0, x) = \begin{cases} (0.45, -0.47, -0.01), & x < 0, \\ (0.04, 0.65, 0.43), & x > 0. \end{cases}$$

Based on this group of initial data, we present some numerical results with $\epsilon = 1$ and $\epsilon = 0.003$ at $t = 0.6$ to indicate the influence of the perturbed parameter ϵ on the formation of vacuum state, please see Figs.6.4-6.5.

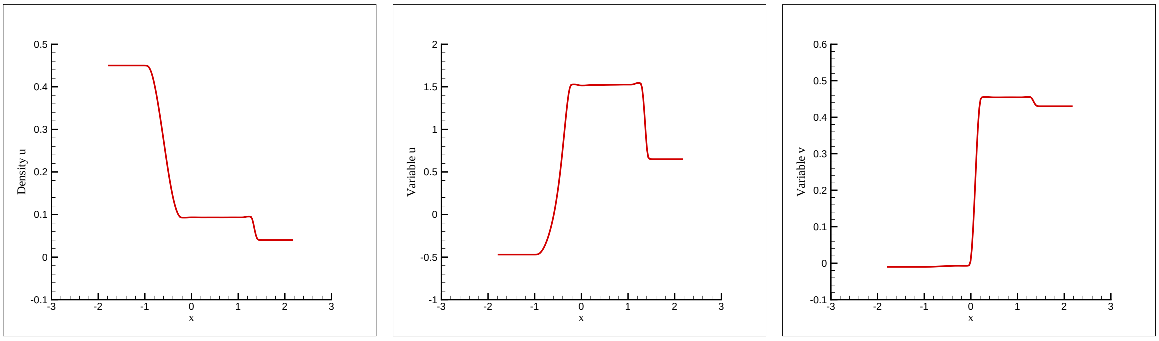

Fig.6.4. Numerical results of ρ, u and v for Data 2 at $\epsilon = 1$.

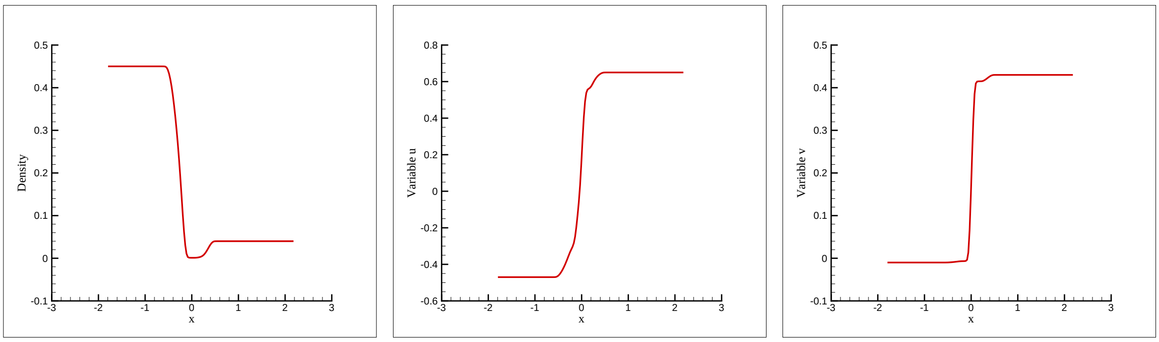

Fig.6.5. Numerical results of ρ, u and v for Data 2 at $\epsilon = 0.003$.

The numerical results in Figs.6.4-6.5 imply that, as ϵ decreases, the intermediate density ρ_*^ϵ infinitely tends to 0, which results in cavitation, and the velocities u and v are closer to two step functions. Thus, the vacuum solution of (1.4) can be obtained as the limit of any solution of (1.1) consisting of two rarefaction waves and possibly one contact discontinuity.

In a word, the numerical results presented above coincide with the theoretical analysis.

References

[1] M. C. Bento, O. Bertolami, A. A. Sen, Generalized Chaplygin gas, accelerated expansion, and dark-energy-matter unification, Phys. Rev. D 66(4) (2002) 043507.

[2] M. C. Bento, O. Bertolami, A. A. Sen, Generalized Chaplygin gas and cosmic microwave background radiation constraints, Phys. Rev. D 67(6) (2003) 063003.

[3] Y. Brenier, E. Grenier, Sticky particles and scalar conservation laws, SIAM J. Numer. Anal. 35 (1998) 2317-2328.

[4] T. Chang, G. Chen, S. Yang, 2-D Riemann problem in gas dynamics and formation of spiral, in: Nonlinear Problems in Engineering and Science—Numerical and Analytical Approach (Beijing, 1991), Science Press, Beijing, 1992, pp. 167-179.

[5] T. Chang, G. Chen, S. Yang, On the Riemann problem for two-dimensional Euler equations. I. Interaction of shocks and rarefaction waves, Discrete Contin. Dyn. Syst. 1 (1995) 555-584.

[6] T. Chang, G. Chen, S. Yang, On the Riemann problem for two-dimensional Euler equations. II. Interaction of contact discontinuities, Discrete Contin. Dyn. Syst. 6 (2000) 419-430.

[7] S. Chaplygin, On gas jets, Sci. Mem. Moscow Univ. Math. Phys. 21 (1904) 1-121.

[8] G. Chen, H. Liu, Formation of delta-shocks and vacuum states in the vanishing pressure limit of solutions to the Euler equations for isentropic fluids, SIAM J. Math. Anal. 34 (2003) 925-938.

[9] G. Chen, H. Liu, Concentration and cavitation in the vanishing pressure limit of solutions to the Euler equations for nonisentropic fluids, Physica D 189 (2004) 141-165.

[10] C. M. Dafermos, Hyperbolic Conversation Laws in Continuum Physics, Grundlehren der mathematischen Wissenchaften, Springer, Berlin-Heidelberg-New York, 2010.

[11] Q. Ding, L. Guo, The vanishing pressure limit of Riemann solutions to the non-isentropic Euler equations for generalized Chaplygin gas, Advances in Mathematical Physics 2019(2) (2019) 1-12.

[12] W. E, Yu.G. Rykov, Ya.G. Sinai, Generalized variational principles, global weak solutions and behavior with random initial data for systems of conservation laws arising in adhesion particle dynamics, Comm. Math. Phys. 177 (1996) 349-380.

[13] L. Guo, W. Sheng, T. Zhang, The two-dimensional Riemann problem for isentropic Chaplygin gas dynamic system, Commun. Pure Appl. Anal. 9 (2010) 431-458.

[14] J. Hu, One-dimensional Riemann problem for equations of constant pressure fluid dynamics with measure solutions by viscosity method, Acta Appl. Math. 55 (1999) 209-229.

[15] G. Jiang, E. Tadmor, Non-oscillatory central schemes for multidimensional hyperbolic conservation laws, SIAM J. Sci. Comput. 19(6) (1998) 1892-1917.

[16] H. Li, Z. Shao, Delta shocks and vacuum states in vanishing pressure limits of solutions to the relativistic Euler equations for generalized Chaplygin gas, Commun. Pure Appl. Anal. 15(6) (2016) 2373-2400.

[17] J. Li, Note on the compressible Euler equations with zero temperature, Appl. Math. Lett. 14 (2001) 519-523.

[18] M. Lin, L. Guo, The limit Riemann solutions to nonisentropic Chaplygin Euler equations, Open Mathematics 18(1) (2020) 1771-1787.

[19] L. Pan, X. Han, The Aw-Rascle traffic model with Chaplygin pressure, J. Math. Anal. Appl. 401(1) (2013) 379-387.

[20] Y. Pang, Delta shock wave with Dirac delta function in multiple components for the system of generalized Chaplygin gas dynamics, Boundary Value Problems 2016 (2016) 202.

[21] Y. Pang, Delta shock wave in the compressible Euler equations for a Chaplygin gas, J. Math. Anal. Appl. 448(1) (2017) 245-261.

[22] M. R. Setare, Interacting holographic generalized Chaplygin gas model, Physics Letters B 654(1) (2007) 1-6.

[23] S.F. Shandarin, Ya.B. Zeldovich, The large-scale structure of the universe: Turbulence, intermittency, structures in a self-gravitating medium, Rev. Modern Phys. 61 (1989) 185-220.

[24] C. Shen, M. Sun, Exact Riemann solutions for the drift-flux equations of two-phase flow under gravity, J. Differential Equations 314 (2022) 1-55.

[25] W. Sheng, G. Wang, G. Yin, Delta wave and vacuum state for generalized Chaplygin gas dynamics system as pressure vanishes, Nonlinear Analysis: Real World Applications 22 (2015) 115-128.

[26] M. Sun, J. Xin, On the delta shock wave interactions for the isentropic Chaplygin gas system consisting of three scalar equations, Filomat 33(16) (2019) 5355-5373.

[27] H. Tsien, Two dimensional subsonic flow of compressible fluids, J. Aeron. Sci. 6 (1939) 399-407.

[28] T. von Karman, Compressibility effects in aerodynamics, J. Aeron. Sci. 8 (1941) 337-365.

[29] G. Wang, The Riemann problem for one dimensional generalized Chaplygin gas dynamics, J. Math. Anal. Appl. 403(2) (2013) 434-450.

[30] G. Yin, K. Song, Vanishing pressure limits of Riemann solutions to the isentropic relativistic Euler system for Chaplygin gas, J. Math. Anal. Appl. 411 (2014) 506-521.

[31] Q. Zhang, The vanishing pressure limit of solutions to the simplified Euler equations for isentropic fluids, Annals of Applied Mathematics 28(1) (2012) 115-126.

[32] T. Zhang, Y. Zheng, Conjecture on the structure of solutions of the Riemann problem for two-dimensional gas dynamics systems, SIAM J. Math. Anal. 21 (1990) 593-630.

[33] Y. Zhang, Y. Pang, J. Wang, Concentration and cavitation in the vanishing pressure limit of solutions to the generalized Chaplygin Euler equations of compressible fluid flow, Eur. J. Mech. B-Fluids 78 (2019) 252-262.

[34] Y. Zhang, Y. Zhang, Interactions of delta shock waves for the equations of constant pressure fluid dynamics, Differential Equations & Applications 13(1) (2021) 63-84.